J Solid State Electrochem (2002) 6: 194–202
DOI 10.1007/s100080100214

ORIGINAL PAPER

D. Gopi · S. Rajeswari

Surface characterization and electrochemical corrosion behaviour of 304 stainless steel in aqueous media

Received: 19 October 2000 / Accepted: 14 March 2001 / Published online: 23 August 2001

Abstract A formulation consisting 100 ppm of 3-phosphonopropionic acid, 50 ppm of Zn^{2+} and 150 ppm of Tween 80 (polyoxyethylene sorbitan monooleate) offered 97.4% inhibition to the corrosion of 304 austenitic stainless steel immersed in a groundwater environment. This formulation functioned as a mixed inhibitor. The protective film was analysed by luminescence, XRD and FTIR spectra and pit morphology and was also observed by scanning electron microscopy.

Keywords Stainless steel · Corrosion inhibition · Phosphonic acid · Zinc · Non-ionic surfactants

Introduction

Pitting corrosion of stainless steel (SS) is of great practical interest. It can be a destructive form of corrosion in engineering structures if it causes perforation of equipment. Most SS equipment failures are caused by chloride ions, especially in cooling water systems.

The cooling water system is one of the major auxiliary supporting service systems for the operation of thermal, nuclear power plant and many industries [1]. Mostly, inland thermal power plants and industries utilize groundwater for cooling purposes. Though groundwater satisfies almost all the conditions of a coolant, the associated problems of scaling and pitting corrosion need extensive attention. Thus the environment makes it necessary to add chemical compounds to the operating fluid to minimize scale formation and pitting attack [2].

D. Gopi (✉) · S. Rajeswari
Department of Analytical Chemistry,
University of Madras, Guindy Campus,
Chennai 600 025, India
E-mail: vandaigopi@yahoo.com
Fax: +91-44-2352494

The mechanisms of inhibition of localized corrosion are quite difficult to establish in view of the complexity of the localized corrosion processes coupled with all of the possible interactions of the inhibitor with surface or interphase chemistry.

Complex formation, interphase inhibition and surface micelle formation effects have been proposed for metals under uniform corrosion conditions [3, 4, 5, 6, 7, 8, 9, 10] and such processes may also be important for the inhibition of localized forms of attack on passive metals. Similar approaches have been reported for the corrosion of SS [11, 12, 13, 14, 15, 16, 17].

The corrosion inhibition of SS in neutral aqueous media is one of the most important tasks for cooling water system operations. Over the past two decades, some phosphonates have been explored owing to their good corrosion inhibition efficiency, scale resistance activity and low toxicity [18, 19, 20, 21, 22, 23, 24]. Bivalent cations like Zn^{2+} are often applied as additives for uniform corrosion conditions. In the presence of bivalent cations the inhibition effect of phosphonic acid in aqueous solution increases synergistically. Hausler [25] has pointed out the possible importance of the formation of an extended phase (interphase inhibition) at the metal/solution interface following initial adsorption of an organic species.

The present work was undertaken to study the phenomena of synergistic corrosion inhibition and optimization of a ternary mixture to achieve maximum inhibition of 304 SS in groundwater. A ternary mixture consisting of 3- phosphonopropionic acid (3-PPA), Zn^{2+} and polyoxyethylene sorbitan monooleate (Tween 80) was used. The synergism was evaluated by open circuit potential (OCP) time measurements, potentiodynamic polarization measurements, crevice corrosion studies and impedance measurements.

The protective film formed on the surface of 304 SS was studied by luminescence spectra, Fourier transform infrared spectra (FTIR) analysis and X-ray diffraction (XRD) studies.

Experimental

Electrochemical cell assembly

Polarization studies were carried out in a conventional three-electrode cell consisting of a platinum counter electrode, a saturated calomel reference electrode (SCE) and the working electrode.

Electrode preparation

The composition of 304 SS used was Cr 18%, Ni 8%, C 0.07%, Mn 1.72%, Si 1.03%, P 0.039% and S 0.016%, with Fe for the balance. The material was cut into pieces 1×1×0.3 cm in size for electrochemical studies. Each piece was attached with a brass rod using silver paste for electrical contact. Then the samples were mounted on an epoxy resin in such a way that only one side with 1 cm^2 surface area was exposed. The mounted samples were polished successively up to 1000 grit SiC emery paper and final polishing was done with 6 μm and 1 μm diamond paste. The samples were degreased with acetone and ultrasonically cleaned using deionized water. This served as the working electrode. Groundwater was used as the electrolyte, whose composition is given in Table 1; the conductivity of groundwater is 1690 μS/cm.

OCP measurements

As soon as the samples were immersed in the electrolyte, the initial potentials of the samples were noted and monitored as a function of time until the potential of the samples reached a steady value. Similarly, the experiments were carried out in the presence of the inhibitors. The structures of the inhibitor compounds used in the study are given in Fig. 1.

Polarization measurements

Polarization measurements were carried out using a Bio-Analytical system electrochemical analyser (BAS), provided with an X-Y recorder. The working electrode was depolarized to –1100 mV for 1 min to remove the native oxides on the surface and was allowed to stabilize for 1 h until a constant potential was reached, which is referred as the corrosion potential (E_{corr}). The cathodic and anodic polarization curves for the 304 SS specimen in the test environment were recorded at a sweep rate of 1 mV/s. In all the cases the potential was changed in the cathodic direction from the corrosion potential to –1200 mV and the electrode was left to attain the corrosion potential. Then the electrode was anodically polarized up to 1600 mV. All the electrochemical experiments were carried out in a nitrogen atmosphere by purging nitrogen gas.

Crevice corrosion studies

The crevice corrosion studies were carried out on the working electrode by creating a crevice using a specially designed glass assembly described by Dayal et al. [26]. The tip of the glass rod was brought into close contact with the electrode surface using a nut and threaded rod arrangement. To determine the critical crevice potential (E_{cc}), the potential was increased from E_{corr} in the noble direction at a scan rate of 1 mV/s until the current increased rapidly.

Table 1 Analysis of groundwater

Species	ppm
Total dissolved salts	1185
Total alkalinity	330
Calcium	131
Magnesium	43
Chloride	279
Sulfate	130

Electrochemical impedance studies

Electrochemical impedance studies were carried out on the system comprising the inhibitors using a Solartron Interface (SI 1285) and Solartron FRA (1255). The polarization resistance and capacitance were calculated using commercial Z view 1.5b software (Scribner Associates).

Surface characterization studies

The 304 SS specimens were immersed in various test solutions for a period of 30 days. After 30 days, the specimens were taken out and dried. The nature of the film formed on the surface of the metal specimens was analysed by various surface analytical techniques.

Luminescence spectra

Luminescence spectra of the film formed on the metal surface were recorded using a Perkin-Elmer LS5B fluorescence spectrophotometer equipped with a pulsed xenon lamp, attached to an IBM PC via an RS-232C interface. The emission spectra were corrected for the spectral response of the photomultiplier tube used.

X-ray diffraction

XRD patterns of the film formed on the metal surface were recorded using a computer-controlled Rigaku-Denki RU 200 diffractometer with Cu K_α (Ni-filtered) radiation ($\lambda = 1.5418$ Å) at a rating of 40 kV and 20 mA. The scan rate was 0.05–20° per step and the measuring time was 1 s per step.

FTIR spectra

The FTIR spectra were recorded using a Perkin-Elmer 1600 FTIR spectrophotometer.

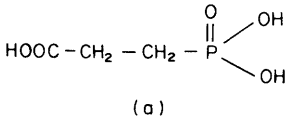

(a)

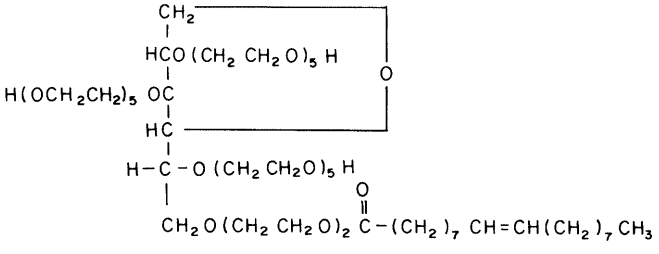

(b)

Fig. 1 The structure of inhibitor compounds: **a** 3-phosphonopropionic acid; **b** Tween 80

Pit morphological studies

After polarization measurements, the electrode was removed from the electrochemical cell, thoroughly washed with distilled water, cleaned with acetone, dried and observed in a scanning electron microscope for the pit morphology. The metallographic examinations of the 304 SS were carried out using a Leica Stereoscan 440 computer-controlled scanning electron microscope.

Results and discussion

OCP versus time measurements

The OCP versus time plots for SS in groundwater are shown in Fig. 2. From the figure it is clear that the presence of 3-PPA shifted the OCP value to the noble (positive) direction, i.e. –12 mV, indicating that the inhibitor controls the anodic reaction. In the presence of Zn^{2+} the OCP value was found to be –187 mV, indicating that it controls the cathodic reaction. Similarly, the presence of Tween 80 also shifted the OCP value towards the more noble region (–72 mV). The combination of 3-PPA (100 ppm) and Zn^{2+} (50 ppm) shifted the OCP value to – 80 mV, thereby indicating that this combination controls both the cathodic as well as the anodic reaction. With the addition of Tween 80 to the above mixture, the OCP value was shifted to –45 mV, indicating that this combination predominantly controls the anodic dissolution of the metals by forming a protective film which is responsible for the minor variations observed in the curves.

Polarization measurements

The cathodic and anodic polarization of 304 SS in groundwater in the presence and absence of various concentrations of inhibitor were carried out. Each inhibitor was studied at eight different concentration levels, e.g. 25, 50, 75, 100, 125, 150, 200 and 250 ppm in the case of 3-PPA and Tween 80 and 10, 20, 30, 40, 50, 60, 80 and 100 ppm in the case of Zn^{2+}. In the case of 3-PPA, the efficiency was found to increase appreciably with the increase in concentration of the inhibitor up to 100 ppm, after which it decreased. Similarly, the optimum concentration of Zn^{2+} and Tween 80 were also evaluated based on inhibition efficiency and were found to be 50 ppm and 150 ppm, respectively. The polarization curves of the optimized concentrations of the inhibitors are given in Fig. 3.

The polarization curves of 3-PPA and the corresponding corrosion parameters are shown in Table 2. The corrosion potential (E_{corr}) of 304 SS was shifted towards the noble direction and a decrease in I_{corr} was noticed with the addition of 3-PPA.

In the presence of Zn^{2+}, the polarization curves were shifted towards the region of lower current density (I_{corr}). From the polarization curves it can be inferred that $Zn(OH)_2$ formed on the metal surface and retards the oxygen reduction reaction, and thus controls the cathodic reaction of the metal. However, the combination consisting of 100 ppm of 3-PPA and 50 ppm of Zn^{2+} reduced the I_{corr} value to 0.120×10^{-2} mA/cm^{-2} and also the breakdown potential (E_b) was shifted towards the noble direction, indicating that the dissolution of the

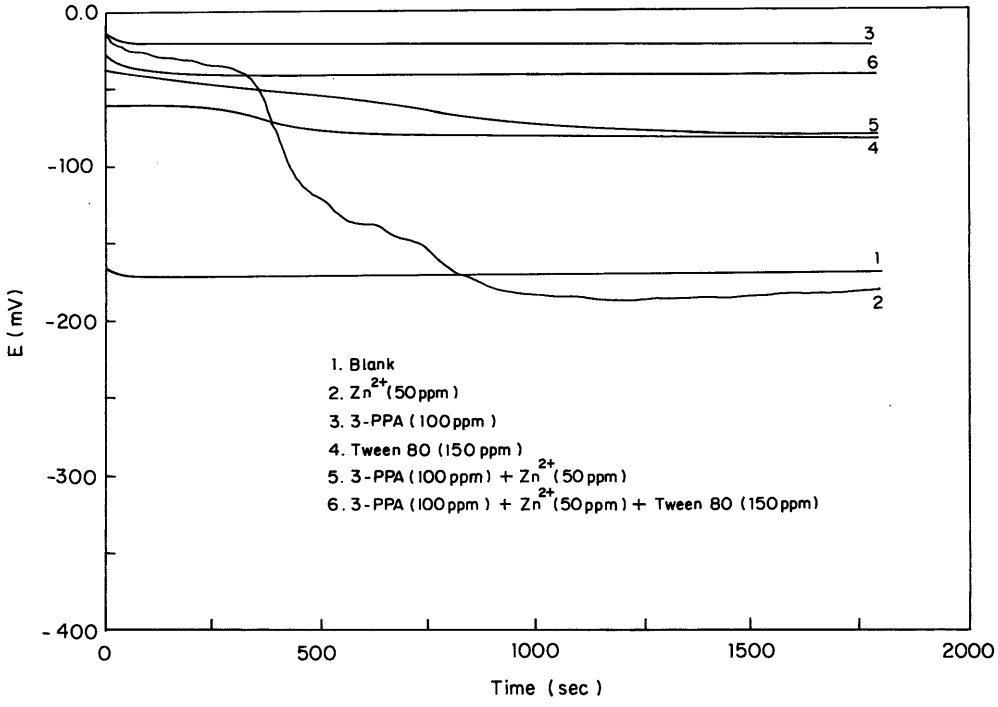

Fig. 2 Variation of open circuit potential with time of 304 SS in groundwater in the presence and absence of inhibitors

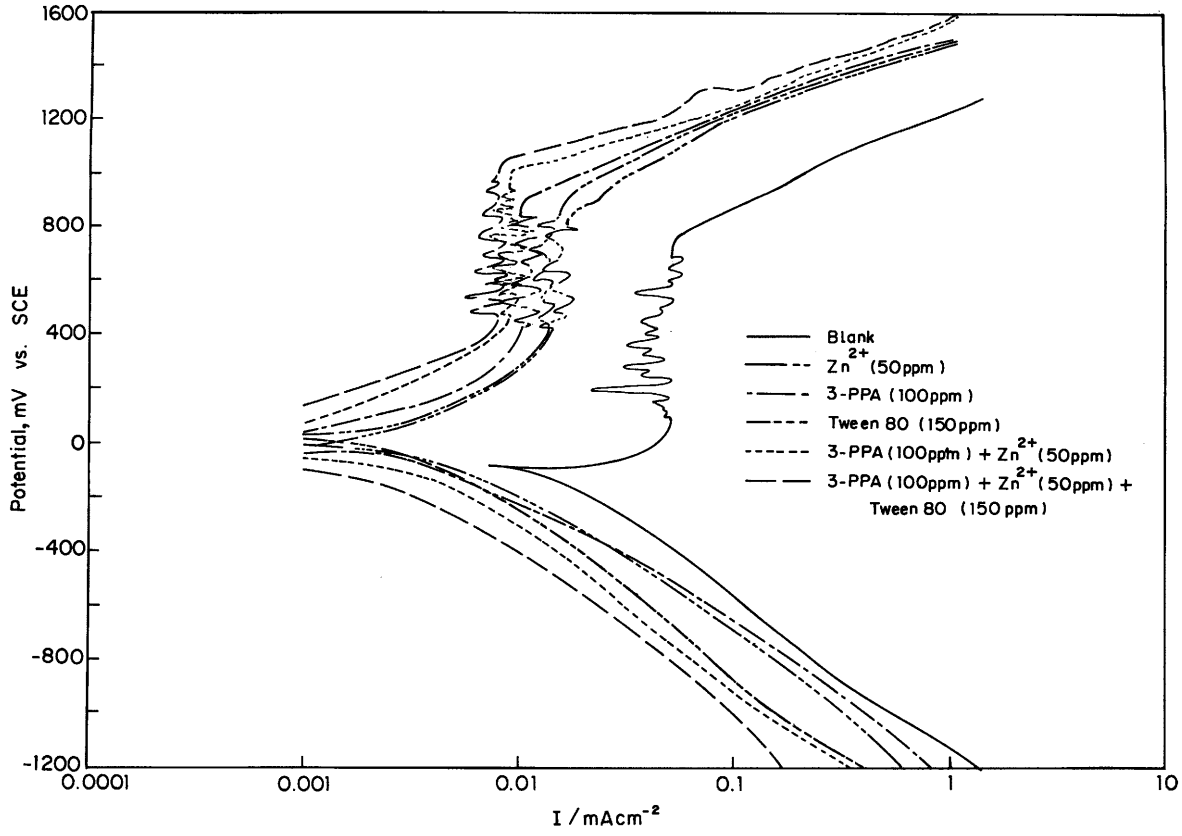

Fig. 3 Polarization curve of 304 SS at different concentration ratios of inhibitors in groundwater

metal was reasonably reduced. There was a further decrease in I_{corr} with the addition of 150 ppm of Tween 80. Thus a powerful synergism of corrosion inhibition was exhibited by the combination of these inhibitors in groundwater.

The synergism s was calculated by using Eq. 1 [27]:

$$s = (i_1 i_2)/(i_{1,2} i_0) \quad (1)$$

where i_1 is the corrosion current density of additive 1, i_2 is the corrosion current density of additive 2, $i_{1,2}$ is the measured current density of additives 1 + 2, and i_0 is the current density for the blank solution. In the case of the ternary system, i_1 is the measured current density of additives 1 + 2, i_2 is the measured current density of additive 3 and $i_{1,2}$ is the measured current density of additives 1 + 2 + 3. The synergism s approaches the value of 1 when no interaction between the inhibitor compounds exists; when $s > 1$, this points to a synergistic effect. In the case of $s < 1$, the antagonistic interaction of inhibitors prevails.

The mechanistic aspects of corrosion inhibition of 304 SS in groundwater by 3-PPA, Zn^{2+} and Tween 80 can be explained in terms of complexation and adsorption, since Zn^{2+} and phosphonic acid are able to form complexes with metal ions.

From the experimental results, the interaction of Zn^{2+} can be described as follows. During the dissolution of iron, the pH increases at the metal/electrolyte interface owing to oxygen reduction. Thus $Zn(OH)_2$ precipitation may take place at the cathodic sites of the electrode surface [27], i.e. the rate of oxygen reduction could be reduced by the formation of insulating $Zn(OH)_2$ on the cathodic area. As reported by earlier

Table 2 Polarization parameters of 304 stainless steel in groundwater in the presence of a combination of inhibitors

Inhibitor	Concentration (ppm)	OCP (mV)	E_{corr} (mV)	$I_{corr} \times 10^{-2}$ (mA cm^{-2})	E_b (mV)	E_{cc} (mV)	IE (%)[a]	Synergism (s)
Blank	–	–171	–76	1.000	790	760	–	–
Zn^{2+}	50	–187	–70	0.370	800	775	66.0	–
3-PPA	100	–012	–05	0.330	902	782	67.0	–
Tween 80	150	–072	–14	0.500	795	772	50.0	–
Zn^{2+} + 3-PPA	50 + 100	–080	–19	0.120	1022	1004	88.0	1.01
Zn^{2+} + 3-PPA + Tween80	50 + 100 + 150	–045	–05	0.026	1048	1033	97.4	2.30

[a]IE = inhibition efficiency

workers, the addition of 3-PPA reduces the metal dissolution reaction. This may be due to adsorption and complex formation of phosphonic acid at the surface of the metal [18, 19, 20, 21, 22, 23, 24].

With the combined application of Zn^{2+} and 3-PPA, the corresponding anodic and cathodic reactions of the metal can be generalized as follows. The local cathodic region was inhibited by Zn^{2+} ions and the local anodic region was inhibited by 3-PPA. The mutual inhibition effect was believed to reduce metal dissolution. In fact, precipitation was observed in the solution containing an inhibitor mixture of $Zn^{2+} + 3$PPA in a 1:2 ratio. This precipitate probably consists of a mixture of polynuclear, slightly soluble Zn^{2+}-PPA complexes and zinc hydroxide.

The Zn^{2+}-PPA complex diffuses from the bulk solution to the surface of the metal and is converted into a Fe^{2+}-PPA complex, which is more stable than Zn^{2+}-PPA [28]. The released Zn^{2+} causes $Zn(OH)_2$ precipitation at the local cathodic sites. Thus the protective film consists of a Fe^{2+}-PPA complex and $Zn(OH)_2$.

More significant synergism was attained by the addition of a non-ionic surfactant like Tween 80 to the $Zn^{2+} + 3$-PPA system. The presence of a long hydrocarbon chain in Tween 80 may induce hydrophobic characteristics and may favour inhibitor dispersibility and limit corrosion, which is evident from the increased inhibition efficiency.

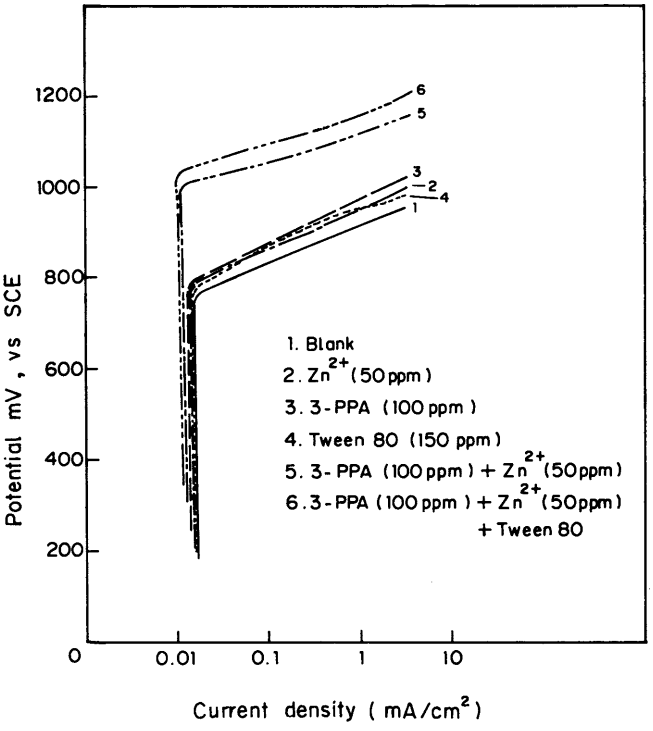

Fig. 4 Crevice corrosion behaviour of 304 SS at different concentration ratios of inhibitors in groundwater

Crevice corrosion studies

The environment prevailing at the actual operating conditions of the cooling circuit involves joints and nuts connected to the material, which results in crevice corrosion attack. Oxygen present in the crevice is consumed quite rapidly during passivation. Owing to this, depletion of oxygen takes place leading to the formation of a concentration cell, which in turn accelerates the crevice corrosion.

The critical crevice corrosion potential values of 304 SS in various inhibitor formulations under study were determined (Fig. 4). The presence of the Zn^{2+} + 3-PPA + Tween 80 system shifted the E_{cc} values towards the more noble direction. Thus the presence of above combination improves the crevice corrosion resistance of 304 SS.

Electrochemical impedance studies

The impedance plots of 304 SS in groundwater with various inhibitors are presented in Fig. 5. The EIS parameters are given in Table 3. An increase in polarization resistance and a decrease in capacitance with the addition of the surfactant Tween 80 to 3-PPA + Zn^{2+} shows better corrosion resistance. The decrease in capacitance is due to the formation of a complex at the metal interface which reduced the thickness of the double-layer charges around the metal surface.

A significant synergistic effect of inhibition was achieved by the addition of a non-ionic surfactant like Tween 80 to the $Zn^{2+} + 3$-PPA system. It can be postulated that the long hydrocarbon part of the Tween 80 ensures a large surface coverage. If the alkyl group is too long, the hydrophobicity of the molecule increases, which obviously promotes the surface activity of the molecule, thus accounting for a considerable increase in the E_b value. Thus the addition of a surfactant to the $Zn^{2+} + 3$-PPA system provides an effective impervious barrier to the dissolution of metal and thus affords protection against corrosion.

Surface characterization

Luminescence spectra

The UV luminescence emission spectra of the solid 3-PPA, iron complex and zinc complex excited at 320 nm are shown in Fig. 6. The solid 3-PPA spectra and solid Zn^{2+} did not exhibit any peaks. The zinc complex and the iron complex exhibited a peak at 465 and 445 nm, respectively. The luminescence spectra of the films formed on the surface of the metal specimen immersed for a period of 30 days in 3-PPA, Zn^{2+} ions and 3-PPA + Zn^{2+} were recorded using an exciting wavelength of 320 nm (Fig. 7). The emission spectra showed a peak at 445 nm, suggesting that the complex formed on the surface is an iron phosphonate complex and not a zinc complex. The intensity of the luminescence spectra of the film formed

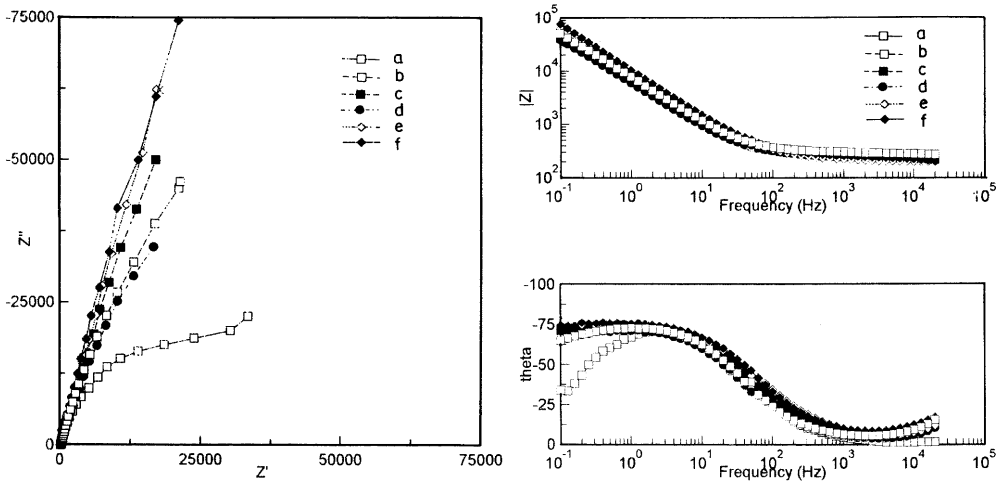

Fig. 5 Bode and Nyquist plot of 304 SS at different concentration ratios of inhibitors in groundwater: *a* blank; *b* Tween 80 ; *c* 3-PPA; *d* Zn^{2+}; *e* Zn^{2+} + 3-PPA; *f* Zn^{2+} + 3-PPA + Tween 80

Table 3 Impedance parameters of 304 stainless steel in the presence of different inhibitor mixtures in groundwater

Inhibitors	Concentration (ppm)	Polarization resistance×10^2 (kΩ/cm^2)	Capacitance (μF/cm^2)
Blank	–	57.38	81.68
Zn^{2+}	50	198.25	77.81
3-PPA	100	235.33	70.76
Tween 80	150	132.32	77.98
Zn^2 + 3-PPA	50 + 100	638.07	64.06
Zn^2 + 3-PPA + Tween80	50 + 100 + 150	3128.05	48.11

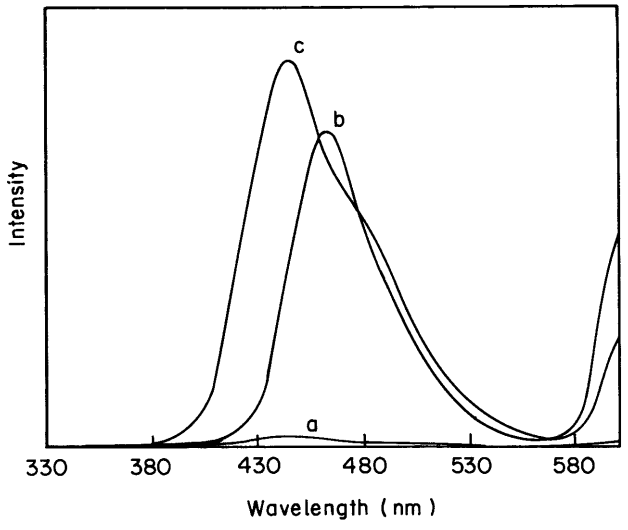

Fig. 6 Luminescence spectra of solids at $\lambda_{ex} = 320$ nm: *a* 3-PPA; *b* Zn^{2+}-3-PPA complex; *c* Fe-3-PPA complex

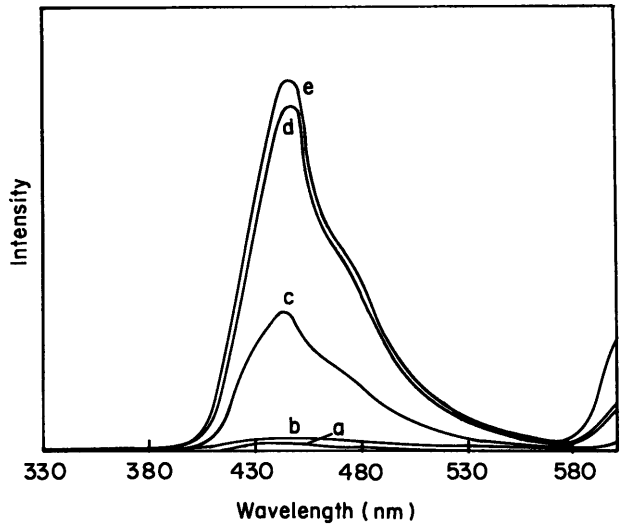

Fig. 7 Luminescence emission spectra of the surface film formed on 304 SS in groundwater at $\lambda_{ex} = 320$ nm: *a* blank; *b* Zn^{2+}; *c* 3-PPA; *d* Zn^{2+} + 3-PPA; *e* Zn^{2+} + 3-PPA + Tween 80

from 3-PPA alone is weak compared to that of the 3-PPA + Zn^{2+} and 3-PPA + Zn^{2+} + Tween 80 systems. It has been postulated that several oxides of iron are formed on the surface of the metal. The composition of these oxides is high that the complex formed between Fe^{2+} and 3-PPA is masked and hence the intensity of the luminescence spectrum is weak (Fig. 7c). In the presence of 3-PPA + Zn^{2+} and 3-PPA + Zn^{2+} + Tween 80 , 88.0% and 97.4% inhibition efficiency were achieved respectively because of the formation of a protective film of a Fe^{2+}-3-PPA complex, which also accounts for an increase in the intensity of the luminescence spectra (Fig. 7d, e).

X-ray diffraction

The XRD patterns of the film formed on the surface of the SS specimens immersed in various test solutions are

given in Fig. 8. The peaks due to iron appear at $2\theta = 44.3°$ and 65.3°. Peaks at $2\theta = 30.4°$, 36° and 62.4° can be assigned to oxides of iron. Thus it is observed that the surface of the metal immersed in groundwater contains iron oxides such as Fe_3O_4 [29]. This indicates that in the groundwater environment the 304 SS specimen has undergone corrosion, leading to the formation of magnetite.

The XRD pattern of the surface of the metal immersed in a solution containing 100 ppm of 3-PPA + 50 ppm of Zn^{2+} is given in Fig. 8b. It is observed that the peaks due to iron occur at $2\theta = 44.4°$ and 64.9°. The peaks corresponding to Γ-FeOOH appear at $2\theta = 36.9°$ and 61.5° [29].

The XRD pattern of the surface of the alloy immersed in the solution containing 100 ppm 3-PPA + 50 ppm Zn^{2+} + 150 ppm Tween 80 is given in Fig. 8c. It is observed that the peaks due to oxides of iron such as Fe_3O_4 and Γ-FeOOH are found to be absent and the peaks due to iron alone are observed at $2\theta = 44.4°$ and 64.9°.

Fourier transform infrared spectra

FTIR spectra of inhibitor mixtures are presented in Fig. 9. Comparison of the Zn^{2+} + 3-PPA mixtures (Fig. 9a) and 3-PPA spectra (Fig. 9b) shows similarities in the position and relative intensities of the bands. The stretching mode of the P = O bond gives rise to a strong band in the region 1320–1140 cm^{-1} as expected [30]. The two prominent bands at 1080 and 930 cm^{-1} are attributed to the PO_3H_2 group of the 3-PPA molecule. The band at 1080 cm^{-1} is assigned to the P-O stretch of the ionic species (PO_3^{3-}) and the other at 930 cm^{-1} is assigned to the P-OH stretch [30, 31]. The band at 930 cm^{-1} is more asymmetrical for the inhibitor mixture than for 3-PPA.

The reflection absorption spectra of the film formed on polished 304 SS is presented in Fig. 10. By comparison with the Zn^{2+} + 3-PPA mixture spectrum (Fig. 9a), a significant increase in the relative intensity is observed for the band in the region of 1100 cm^{-1}. The band at 930 cm^{-1} almost disappears. This result can be interpreted by interactions of free P-O^- with metallic species

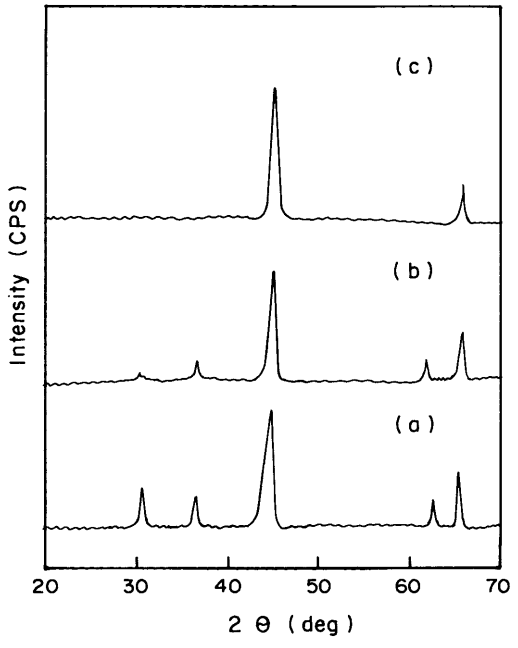

Fig. 8 XRD patterns obtained on the surface film formed on 304 SS at the end of 30 days in different environments: *a* blank; *b* Zn^{2+} + 3-PPA; *c* Zn^{2+} + 3-PPA + Tween 80

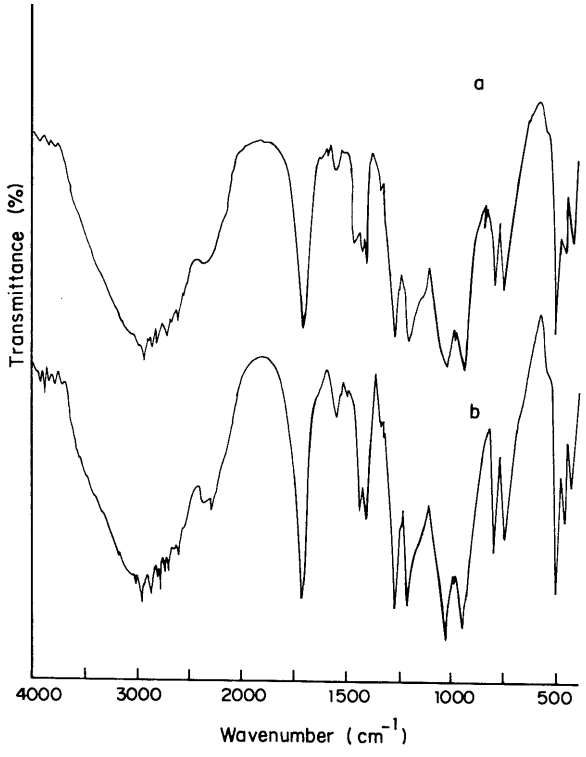

Fig. 9 Infrared transmission spectra of: *a* 3-PPA; *b* Zn^{2+} + 3-PPA

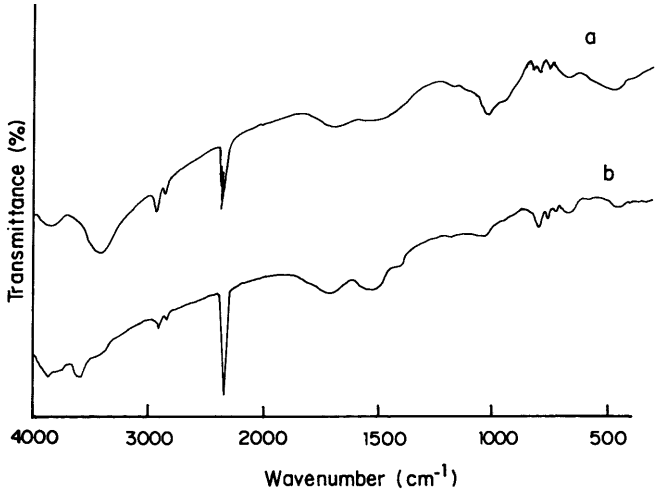

Fig. 10 Infrared reflection-absorption spectrum of the film formed on the 304 SS substrate after immersion in the solution containing the inhibitor mixture: *a* 3-PPA + Zn^{2+}; *b* Zn^{2+}

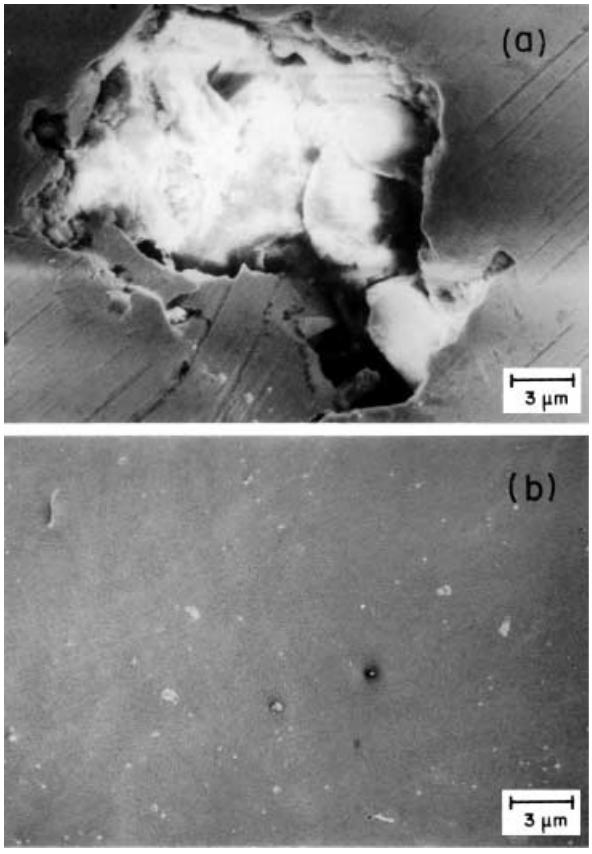

Fig. 11 Pit morphology of 304 stainless steel: (**a**) uninhibited surface; (**b**) inhibited surface

to form P-O-M bonds. Carter et al. [32] found that an IR spectrum obtained with an organic phosphate on a steel substrate was consistent with a reaction of the phosphate with the steel to produce a metal salt. The fact that the band at 930 cm^{-1} due to P-OH stretching is weak further indicates the possibility of a P-O-M (P-O-Fe) bond.

In addition, the spectrum obtained on steel also shows some small bands in the 760–960 cm^{-1} region. For an interpretation of these bands, the FTIR reflection spectrum of the inhibitor mixture was compared with the spectrum obtained for a SS sample immersed in a solution containing only Zn^{2+}. As previously mentioned, the corrosion inhibition of steel by Zn^{2+} leads to the formation of $Zn(OH)_2$ [33]. The bands around 850 cm^{-1} could be assigned to the Zn-OH bending mode. The substitution of an OH group by a halogen shifts the Zn-OH bending mode to lower frequencies [33]. Nevertheless, the presence of different bands in the region 780–850 cm^{-1} suggests the formation of compounds of complex structure such as $Zn_x(OH)_y(Cl)_z$ [33].

Pit morphological studies

The pit morphology of the 304 SS material under study is shown in Fig. 11. Figure 11a shows the pitted region of 304 SS. In the case of the inhibited surface (Fig. 11b), a few pits of very small size were found compared to the blank.

Conclusions

A formulation consisting of 3-PPA, Zn^{2+} and Tween 80 can be used as a potent inhibitor to prevent the pitting and crevice corrosion attack of 304 SS in a neutral aqueous media.

1. The a.c. and d.c. measurements indicate the dependence of the concentration of the inhibitors on the corrosion process.
2. A significant synergism was attained by the combined application of 3-PPA + Zn^{2+} + Tween 80 of 1:0.5:1.5 ratio.
3. The FTIR spectrum obtained on 304 SS is consistent with the reaction of the phosphonic acid with the zinc hydroxide and iron oxide to produce metal salts.
4. The application of a non-ionic surfactant to the Zn^{2+} + 3-PPA system provides an effective impervious barrier to the dissolution of metal and thus affords enhanced protection against pitting and crevice corrosion.

Acknowledgements Financial support by the University Grants Commission (UGC), New Delhi, is gratefully acknowledged.

References

1. Strauss SD, Puckorious PR (1984) Power June:S1
2. Deberry DW, Peyton GR, Clark WS (1984) Corrosion 40: 250
3. Falewicz P, Kuczkowska K (1992) Werkst Korros 43:43
4. Zocher G, Zashch (1990) Metals 26:664
5. Gunasekaran G, Palniswamy N, Apparao BV, Muralidharan VS (1997) Electrochim Acta 49:1427
6. Weisstuch A, Carter DA, Nathan CC (1971) Mater Prot Perform 10:11
7. Schmitt G (1984) Br Corros J 19:165
8. Trabanelli G (1984) Br Corros J 19:150
9. Trabanelli G (1991) Corrosion 47:410
10. Sekine , Hirakawa Y (1986) Nat Assoc Corros Eng 42:5
11. Latha G, Rajeswari S (1996) Anti-Corros Methods Mater 43:19.
12. Lakatos-Varsanyi , Falkenberg F, Olefjord I (1998) Electrochim Acta 43:187
13. Singh A, Chaudhary (1995) J Electochem Soc India 44(2):77
14. Lu KH, Duquette DJ (1990) Corrosion 46:994
15. Shoesmith DW, Mancey DS, Doern DC, Bailey MG (1989) Corrosion 45:149
16. Latha G, Rajeswari S (2000) Corros Rev 18:429
17. Latha G, Rajeswari S (1996) J Mater Eng Perform 5:577
18. Kalman E, Varhegyi B, Bako I, Felhosi I, Karman FH, Shabar A (1994) J Electrochem Soc 14:3357
19. Karman FH, Kalman E, Varallyai L, Konya J (1991) Z Naturforsch 469:183
20. Veres A, Reinhard G, Kalman E (1992) Br Corros J 27:147
21. Ferreday D, Mitcell PJ, Wilcox GD, Greaves B (1993) Br Corros J 28:185
22. Jang JL, Li Y, Ye XR, Wang ZW, Liu Q (1993) Corrosion 49:266

23. Rajendran S, Apparao BV, Palaniswamy N (1999) Anti-Corros Methods Mater 46:284
24. Kalman E (1994) Corrosion inhibitors. (EFC no. 11) Institute of Materials, London
25. Hausler RH (1979) In: Brubaker GR, Phipps BO (eds) Corrosion chemistry. (ACS symp ser 89) American Chemical Society, Washington, p 262
26. Dayal RK, Parvathavarthini N, Gnanamoorthy JB (1983) Br Corros J 18:184
27. Felhosi I, Keresztes Zs, Karman FH, Mohai M, Bertoti I Kalman E (1999) J Electrochem Soc 146:961
28. Rajendran S, Apparao BV, Palaniswamy N (1998) Anti-Corros Methods Mater 45:338
29. Favre M, Landolt D (1993) Corros Sci 34:1481
30. Colthup NB, Daly LH, Wiberley SE (1990) Introduction to infrared and Raman spectroscopy, 3rd edn. Academic Press, New York
31. Gonzlez Y, Lafont MC, Pebere N, Chatainier G, Roy J, Bouissou T (1998) Corros Sci 37:1823
32. Carter RO III, Gierczak CA, Dickie RA (1986) Appl Spectrosc 40:649
33. Srivastava OK, Secco EA (1967) Can J Chem 45:585